ELSEVIER

Journal of Molecular Catalysis A: Chemical 167 (2001) 217–224

JOURNAL OF MOLECULAR CATALYSIS A: CHEMICAL

www.elsevier.com/locate/molcata

An inelastic neutron scattering study of the interaction of dihydrogen with the cobalt site of a cobalt aluminophosphate catalyst Two-dimensional quantum rotation of adsorbed dihydrogen

A.J. Ramirez-Cuesta [a,b,*], P.C.H. Mitchell [a], S.F. Parker [c]

[a] *Department of Chemistry, University of Reading, Reading RG6 6AD, UK*
[b] *Departamento de Fisica, Universidad Nacional de San Luis, 5700 San Luis, Argentina*
[c] *ISIS Facility, Rutherford Appleton Laboratory, Chilton, Didcot, Oxon OX11 0QX, UK*

Received 6 April 2000

Abstract

Analysis of the inelastic neutron scattering (INS) spectrum of dihydrogen adsorbed at the cobalt site of a cobalt aluminophosphate (CoAlPO) catalyst shows that weakly bound dihydrogen is constrained to rotate with the molecular axis aligned with the electric field in the cavity and a more strongly bound species in a plane parallel to the surface. Hydrogen adsorbed on the Al^{3+} sites behaves as a slightly hindered three-dimensional rotor. © 2001 Elsevier Science B.V. All rights reserved.

Keywords: Neutron scattering; Electric field; Cobalt site

1. Introduction

As part of a continuing study [1,2] of the binding and activation of dihydrogen at catalytic centres and hydrogen atom spillover, we report the interaction of H_2 with the cobalt site of cobalt aluminophosphate (CoAlPO-18) [3–7]. Cobalt containing microporous materials are important selective oxidation catalysts in, for example, liquid-phase oxidation of alkenes with dioxygen [8,9] and selective oxidation of cyclohexane to cyclohexanone [10]. The synthesis of the CoAlPO-18 catalyst is accomplished by standard hydrothermal sol–gel techniques [11]. Removal of the template is effected by calcination in oxygen; the cobalt(II) is oxidised to cobalt(III) [12]. The catalyst is subsequently reduced in hydrogen to generate Bronsted acid sites. The interaction of the hydrogen molecule with the Co(III) centre is therefore, crucial. The CoAlPO provided the opportunity to study the binding and activation of the H_2 molecule at a well defined site. Here we report a study of the interaction of the H_2 molecule with the Co(III) site, experimentally with inelastic neutron scattering (INS) on the TOSCA spectrometer at the Rutherford Appleton Laboratory, and theoretically with density functional theory calculations (DFT) and perturbation theory. The INS spectrum (energy loss vibrational spectrum) of the bound H_2 molecule enables us to observe and assign the H_2 rotational transitions and to model the H_2 interactions.

* Corresponding author.
E-mail address: a.j.ramirez-cuesta@reading.ac.uk (A.J. Ramirez-Cuesta).

1381-1169/01/$ – see front matter
PII: S1381-1169(00)00509-4

2. Inelastic neutron scattering spectra

In an INS experiment we observe a spectrum of scattered neutron intensity versus energy transfer between the incident neutrons and the scattering nucleus. The neutron experiences energy transfer (1) and momentum transfer (2)

$$\hbar\omega = (E_\mathrm{f} - E_\mathrm{i}) = \frac{\hbar}{2m}(k_\mathrm{f}^2 - k_\mathrm{i}^2) \quad (1)$$

$$h\boldsymbol{Q} = \hbar(\boldsymbol{k}_\mathrm{f} - \boldsymbol{k}_\mathrm{i}) \quad (2)$$

where E, $\boldsymbol{k}$ and m are the energy, wave vector and mass of the neutron, respectively; i and f refer to the initial and final states of the neutron. The neutron spectrum is characterised by the range of ω and $\boldsymbol{Q}$ over which measurements are made [13–15].

The total neutron scattering cross-section is the sum of an incoherent and a coherent contribution:

$$\frac{\mathrm{d}^2\sigma}{\mathrm{d}\Omega\,\mathrm{d}\varepsilon} = \left(\frac{E_\mathrm{f}}{E_\mathrm{i}}\right)^{1/2} [a_\mathrm{inc}^2 S_\mathrm{inc}(\boldsymbol{Q}, \omega) + a_\mathrm{coh}^2 S_\mathrm{coh}(\boldsymbol{Q}, \omega)] \quad (3)$$

where a is the scattering length and $S(\boldsymbol{Q}, \omega)$ is the dynamic structure factor. For most elements appreciable coherent scattering is usually present, but for hydrogen it is the incoherent scattering that dominates and since the scattering cross-section for hydrogen (80 b) is much greater than for other elements ($\leq$5 b), the hydrogen scattering dominates any INS spectrum. At low temperatures $\mathrm{d}^2\sigma/\mathrm{d}\Omega\,\mathrm{d}\varepsilon$ is proportional to the density of states, $g(\omega)$, and the incoherent spectrum can therefore, be used as a direct measure of the density of states [13,15].

INS measurements on the compound CoAlPO-18 (15.7 g in a standard stainless steel INS cell) were made on the TOSCA instrument at the ISIS Facility at the Rutherford Appleton Laboratory [16]. The CoAlPO-18 was heated in oxygen at 773 K (to ensure complete conversion of Co to Co(III), dehydration and removal of the template) and dosed in situ with hydrogen at 20 K to a concentration of ca. $1H_2$ per cavity.

3. Computational methods

Our aim was to compute the rotational modes of the sorbed H_2 molecule constrained by interactions within the internal space of the CoAlPO-18. We used perturbation theory calculations to fit the INS spectrum by a constraining potential and DFT to study at the atomistic level the interaction of the H_2 molecule with components of the catalyst.

3.1. Perturbation calculations

As the out-of-plane forces securing the H_2 to the surface increase in strength the molecule becomes more constrained. Ultimately these rotational states will, themselves, become hindered [17]. The total energy of the system can be expanded as

$$V(z, \theta, \phi) = V_0 + K(z - z_0)^2 + V(\theta, \phi)$$

where K is the spring constant, $z - z_0$ is the vertical displacement of the molecule form its minimum energy position in the harmonic approximation. Within this approximation, the Schrodinger equation remains separable into translational and orientational terms. If we just consider the orientational terms, a general expression for a potential that governs the rotation of the molecule is, in spherical polar coordinates [18]

$$V(\theta, \phi) = \sin^2\theta[a + b\cos(2\phi)] \quad (1)$$

where θ is the polar angle (the angle between the H–H bond and the surface normal), ϕ the azimuthal angle (between the horizontal axis and the projection of the radius vector on the horizontal plane), a and b give the relative weight of the hindrance in both angles. When $b \approx 0$ and $a \leq 0$ the molecule is, at equilibrium, oriented parallel to the surface. In the extreme case for large negative values of b the molecule is effectively constrained to rotate in a plane parallel to the surface; we call this a two-dimensional rotor (2D rotor). If on the other hand the values of b have large positive values the molecule is constrained to remain perpendicular to the surface and we call it a one-dimensional case (1D).

The orientational component of the Schodinger equation was solved treating the orientational potential as a perturbation. The Schodinger equation was solved perturbatively by expansion of the potential in the wavefunctions of the unperturbed H_2 molecule (the spherical harmonics). The resultant matrix was diagonalised numerically to determine the energy states of the perturbed rotor. We used 64 levels in order to have an error of $10^{-5}B$ in the calculated energies.

3.2. Density functional theory calculations

The Co(III) centre was modelled as a distorted tetrahedral $Co(OH)_3OH_2$ neutral cluster [19] with the Amsterdam density functional (ADF) program [20,21] with the generalised gradients approximation, the exchange correlation corrections of Perdew and Wang [22], spin unrestricted calculations and double $\zeta+$ polarisation basis set including relativistic corrections [23]. The cobalt(III) was high spin (four unpaired electrons). The structure was fully relaxed, starting with a fully symmetric tetrahedral arrangement of the Co–O bonds. The optimised cluster geometry was fixed and a hydrogen molecule was added. The total energy of the system was calculated as a function of distance between the H_2 centre of mass and the cobalt centre for different orientations of the molecule relative to the surface normal. The H–H bond distance was allowed to relax to its optimal distance at every simulation step. The main objective of the calculations is to rationalise the adsorption site on the Co centre, i.e. to determine whether the adsorbed H_2 tends to lie parallel to the surface or perpendicular to it.

The Al centre was modelled as an AlO_4 tetrahedron in the same way as the Co site, using the same level of theory and starting with a symmetric tetrahedral arrangement.

4. Results and discussion

4.1. Rotational transitions of the H_2 molecule

Since hydrogen nuclei are fermions, because of the Pauli principle, the total wavefunction (nuclear and rotational) has to be antisymmetric. The ground state, parahydrogen (p-H_2), combines an antisymmetric nuclear spin wavefunction (spin paired $\uparrow\downarrow$) and a symmetric rotational wavefunction. Therefore, the allowed rotational states of parahydrogen are those with even J (the rotational quantum number) including $J = 0$. Conversely the first rotational state, $J = 1$, orthohydrogen (o-H_2), combines a symmetric nuclear spin wavefunction (spin parallel $\uparrow\uparrow$), and an antisymmetric rotational wavefunction; only odd J states are permitted. Conversion of p-H_2 to o-H_2 requires a spin flip mechanism.

Pure rotational transitions of symmetrical diatomic molecules like dihydrogen are forbidden in IR spectroscopy by the dipole selection rule but are readily observed by INS spectroscopy where dipole selection rules do not apply. Thus for p-H_2, from $J = 0$ the ground state, transitions within its manifold are controlled by the coherent cross section of hydrogen, 1.8 b (1 b $= 10^{-28}$ m^2). However, transitions to $J =$ odd states involve a spin exchange with the neutron and are controlled by the incoherent cross section,

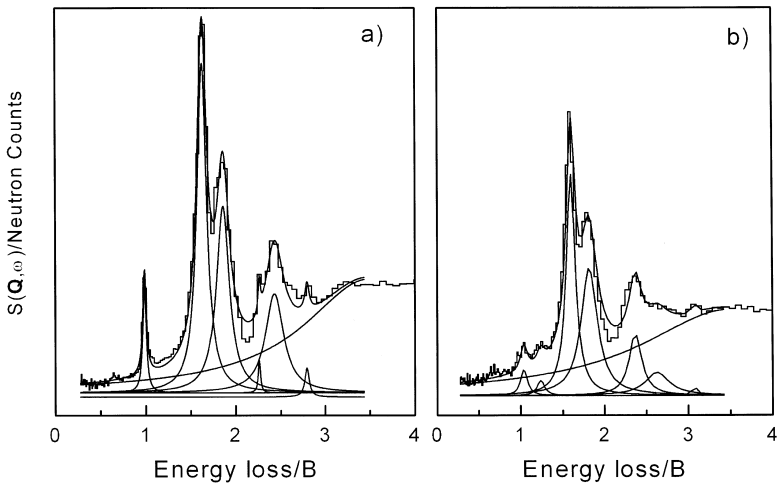

Fig. 1. Inelastic neutron scattering spectrum of H_2 in CoAlPO-18 showing the rotational modes. The peaks are deconvoluted as Lorentzians. (a) Before desorption and (b) after desorption of weakly bound H_2.

Table 1
Assignment of the rotational modes in the INS spectrum of H_2 in CoAlPO-18

Peak position/*B*	Relative area	Width/*B*	Transition	Assignment
0.98	0.125	0.05	$\|0,0\rangle \rightarrow \|1,0\rangle$	1D rotor
1.62	1.000	0.13	$\|0,0\rangle \rightarrow \|1,1\rangle$	2D rotor Al site
1.82	0.896	0.17	$\|0,0\rangle \rightarrow \|1,-1\rangle$	
2.26	0.055	0.03	$\|0,0\rangle \rightarrow \|1,0\rangle$	
2.41	0.584	0.25	$\|0,0\rangle \rightarrow \|1,0\rangle$	
2.80	0.116	0.06	$\|0,0\rangle \rightarrow \|1,1\rangle$	1D rotor

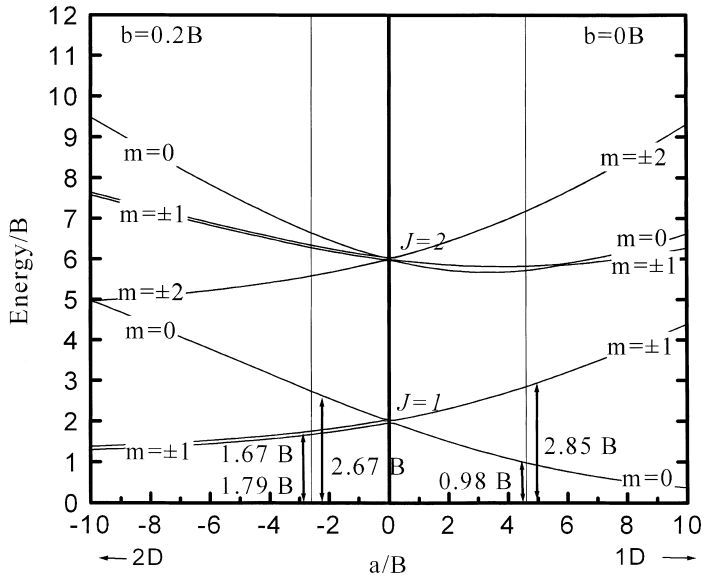

Fig. 2. Rotational states of constrained H_2: energy in units of the rotational constant *B* vs. the perturbation parameter *a* of Fig. 1 with $b = 0.2B$. Vertical arrows locate peaks in the INS spectrum.

79.7 b. This is the reason why there is a very significant intensity for the $J = 0 \rightarrow 1$ feature in the spectra.

The INS spectra (0–350 cm^{-1}) before and after hydrogen desorption are shown in Fig. 1(a) and (b). In this region we observe sharp rotational transitions of the H_2 molecule and a broad recoil tail. The peaks have been fitted as Lorentzians. We refer first to the spectra of solid dihydrogen and physisorbed hydrogen.

Table 2
Assignment of the rotational modes remaining in the INS spectrum of H_2 in CoAlPO-18 after desorption of weakly bound (1D rotor) dihydrogen at 30 K

Peak position/*B*	Relative area	Width/*B*	Transition	Assignment
1.04	0.085	0.09	$\|0,0\rangle \rightarrow \|1,1\rangle$	2D rotor Co Site
1.24	0.044	0.10	$\|0,0\rangle \rightarrow \|1,-1\rangle$	
1.60	0.970	0.13	$\|0,0\rangle \rightarrow \|1,1\rangle$	2D rotor Al Site
1.81	1.000	0.23	$\|0,0\rangle \rightarrow \|1,-0\rangle$	
2.36	0.370	0.28	$\|0,0\rangle \rightarrow \|1,0\rangle$	
3.07	0.038	0.04	$\|0,0\rangle \rightarrow \|1,0\rangle$	2D rotor Co Site

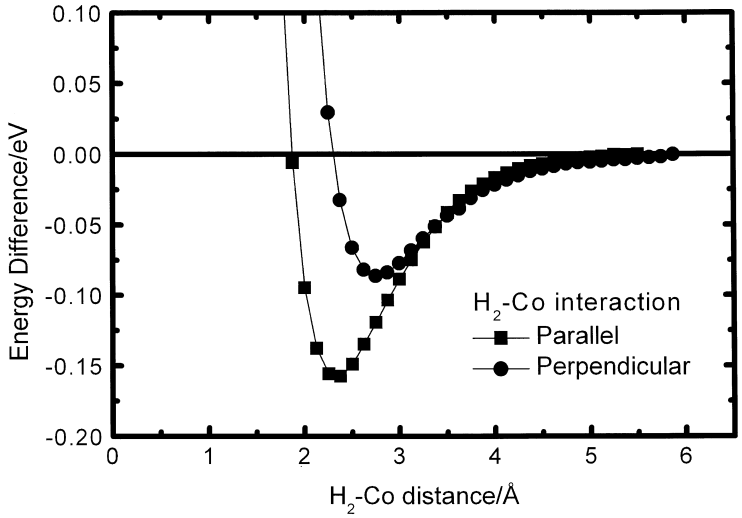

Fig. 3. The potential energy difference as a function of the H_2–Co distance as the hydrogen molecule approaches the $Co(OH)_3OH_2$ cluster with the H–H bond, respectively, parallel and perpendicular to the surface. The energy reference is at a Co–H distance of 6 Å.

4.2. The H_2 molecule as an unconstrained linear rotor

Dihydrogen is an almost free rotor in the solid state and in the ground state has a fully spherical distribution [24]. Molecules rotate freely with almost the same value for the rotational constant as in the gas phase $B = 59.6\,\mathrm{cm}^{-1}$. The energy level scheme is that of a linear rotor in three-dimensional space (3D rotor)

$$E_J = J(J+1)B$$

For dihydrogen adsorbed on graphite, the rotational states are slightly hindered but they can still be represented as perturbed three-dimensional rotor states [25–28]. The rotational ground state is nearly pure $J = 0$. The lowest band of excited states, nominally $J = 1$,

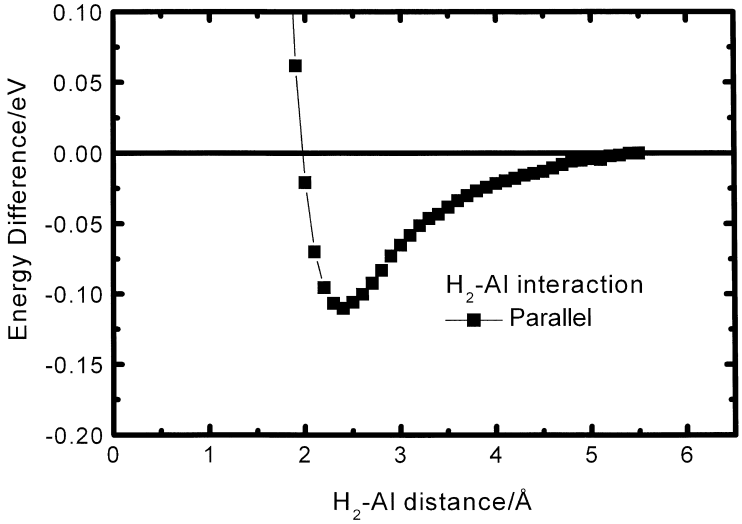

Fig. 4. Mulliken charges on the Co and H atoms as the H_2 molecule approaches the Co centre.

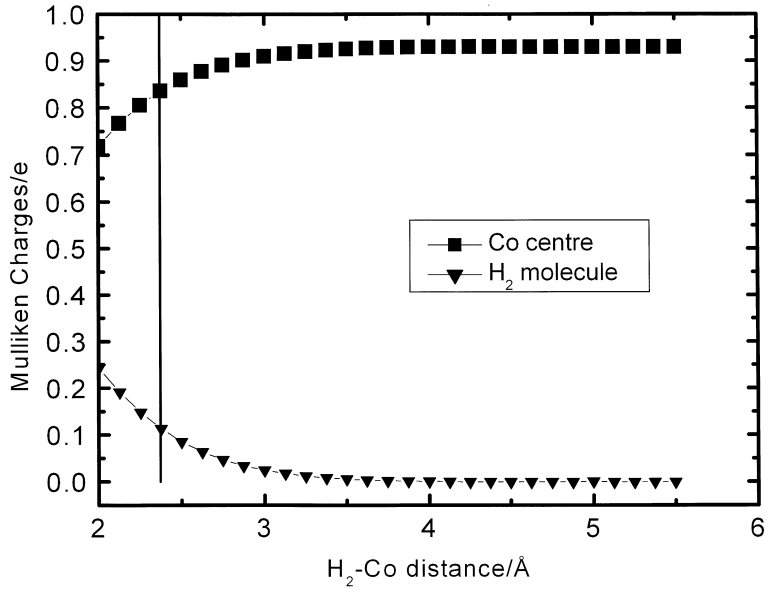

Fig. 5. The potential energy difference as a function of the H_2–Al distance as the hydrogen molecule approaches the AlO_4 cluster with the H–H bond, respectively, parallel and perpendicular to the surface. The energy reference is at a Al–H distance of 6 Å.

are separated from the ground state by an average energy of $2BJ$ and are split by about 20.2–21.8 cm^{-1}. In our previously reported INS spectrum of H_2 on a Ru/C catalyst the lowest energy transition was seen as a sharp strong band at 120 cm^{-1}, $B = 60\,cm^{-1}$ [1]. This was the J (0–1) rotational transition (p- to o-H_2, allowed in INS although strongly forbidden in photon spectroscopy) [29]. It is striking however, that in the spectrum of H_2 adsorbed on CoAlPO (Fig. 1(a)) the lowest energy band is at 58.4 cm^{-1}, generally a featureless region of the spectrum. Clearly we cannot treat all our sorbed H_2 as an unconstrained 3D rotor.

4.3. The H_2 molecule as a constrained linear rotor

In Table 1 we present the effect of the perturbation in the energy transitions from the ground level. We highlight the transitions that appear in the spectrum shown in Fig. 1(a), the assignment of the transitions responsible for these peaks for this spectrum is shown in Table 1. In Figs. 1 and 2(b) we show the spectrum of dihydrogen on CoAlPO after desorption of the very weakly adsorbed species (they desorb at 30 K) and we can observe the disappearance of the peaks assigned to the 1D rotor. There are new peaks that become evident as we desorb these very weakly adsorbed species; the new peaks appear at 1.04, 1.24 and 3.05B in Table 2 we show the peaks that remain and the assignments.

4.4. Modelling the H_2 interaction with the cobalt centre

From the DFT calculations we found that dihydrogen is hindered to rotate in a plane (2D rotor) when adsorbed on the Co centre; we estimate the values of the constants $a \approx 17B$ and $b \approx 0.4B$. If we fit the observed values to the calculations from perturbation theory, we found that the values that give the proper energy transitions to compare with experiment are: $a \approx 21B$ and $b \approx 0.2B$. The result is quite consistent with the observed spectra.

In Fig. 3 we show the potential energy difference as a function of the H_2–Co distance as the hydrogen molecule approaches the $Co(OH)_3OH_2$ cluster with the H–H bond, respectively, parallel and perpendicular to the surface. The energy reference is at a Co–H distance of 6 Å. At the energy minimum the H–H molecule is parallel with the surface at an equi-

librium distance of 2.375 Å; Co–H is 2.406 Å. The H–H distance is 2% longer than that calculated for the molecule at 6 Å from the Co centre. From a Mulliken charge calculation, at the equilibrium distance we find a 0.1*e* transfer of charge from the H_2 to the Co^{3+}, Fig. 4. Clearly the interaction of the H_2 molecule with the CoAlPO weakens the H–H bond.

4.5. Modelling the H_2 interaction with the aluminium centre

The final configuration of the cluster was not distorted. From the study of the energy of the system as a function of the H–Al distance, we found that the H_2 molecule adsorbs more weakly to the Al site (Fig. 5).

5. Conclusions

From our INS spectra and calculations on a model structure we conclude that the H_2 molecule interacts with CoAlPO through the Co(III) centre. Both H atoms are involved and the molecule acts as a single axis rotor. The combination of experiment, theory and simulation proved to be very successful, the experimental results can be analysed in more detail with the help of calculations, in particular, DFT calculations pointed to the region of the spectra to look for evidence of the adsorption of di-hydrogen.

The adsorption of dihydrogen on Co and it behaviour as a 2D rotor is related with the catalytic activity of the Co centre in this material: there is a weakening of the H–H bond in the molecule at the Co centre and it is a precursor to H_2 dissociation.

Acknowledgements

We thank the EPSRC for funding (GR/M90627) and access to the ISIS neutron beam (GR/L13834); Prof. Richard Catlow for his interest; Dr. P. Barrett for providing the CoAlPO-18 and Dr. G. Sankar (Royal Institution) for helpful comments on the CoAlPO structure; Dr. J. Tomkinson (ISIS) for discussion of the hydrogen INS. Dr. John Turner (Royal Institution) was involved in the initial planning of the project.

References

[1] P.C.H. Mitchell, S.F. Parker, J. Tomkinson, D. Tompsett, J. Chem. Soc., Faraday Trans. 94 (1998) 1489.
[2] A.J. Ramirez-Cuesta, P.C.H. Mitchell, S.F. Parker, P. Barrett, J. Chem. Soc., Chem. Commun. 14 (2000) 1257–1258.
[3] H.F.W.L. van Breukelen, M.E. Gerritsen, V.M. Ummels, J.S. Broens, J.H.C. van Hooff, Stud. Surf. Sci. Catal. 105 (1997) 1029.
[4] M. Hartmann, L. Kevan, Chem. Rev. 99 (1999) 635.
[5] T. Maschmeyer, R.D. Oldroyd, G. Sankar, J.M. Thomas, I.J. Shannon, J.A. Klepetko, A.F. Masters, J.K. Beattie, C.R.A. Catlow, Angew. Chem. Int. Ed. Engl. 36 (1997) 1639.
[6] P.A. Barrett, G. Sankar, C.R.A. Catlow, J.M. Thomas, J. Phys. Chem. 100 (1996) 8977.
[7] J.M. Thomas, G.N. Greaves, G. Sankar, P.A. Wright, J. Chen, A.J. Dent, L. Marchese, Angew. Chem. Int. Ed. Engl. 33 (1994) 1871.
[8] H.F.W.L. van Breukelen, M.E. Gerritsen, V.M. Ummels, J.S. Broens, J.H.C. van Hooff, Stud. Surf. Sci. Catal. 105 (1997) 1029.
[9] M. Hartmann, L. Kevan, Chem. Rev. 99 (1999) 635.
[10] T. Maschmeyer, R.D. Oldroyd, G. Sankar, J.M. Thomas, I.J. Shannon, J.A. Klepetko, A.F. Masters, J.K. Beattie, C.R.A. Catlow, Angew. Chem. Int. Ed. Engl. 36 (1997) 1639.
[11] P.A. Barrett, G. Sankar, C.R.A. Catlow, J.M. Thomas, J. Phys. Chem. 100 (1996) 8977.
[12] J.M. Thomas, G.N. Greaves, G. Sankar, P.A. Wright, J. Chen, A.J. Dent, L. Marchese, Angew. Chem. Int. Ed. Engl. 33 (1994) 1871.
[13] J. Li, J. Tomkinson, in: P. Balbuena, J. Seminario (Eds.), Molecular Dynamics, from Classical to Quantum Methods, Elsevier, Amsterdam, 1999, p. 471.
[14] J. Li, J. Chem. Phys. 105 (1996) 6733.
[15] H. Zabel, in: E. Baruchel (Ed.), Neutron and Synchrotron Radiation for Condensed Matter Studies, Vol. I, Springer, Berlin, 1994.
[16] S.F. Parker, C.J. Carlile, T. Pike, J. Tomkinson, R.J. Newport, C. Andreani, F.P. Ricci, F. Sachetti, M. Zoppi, Phys. B (1998) 241–243.
[17] D. White, Lassettre, J. Chem. Phys. 32 (1960) 72.
[18] A.P. Smith, R. Benedeck, F.R. Trouw, M. Minkoff, L.H. Yang, Phys. Rev. B 53 (1996) 10187.
[19] D. Farcasiu, P. Lukinskas, J. Phys. Chem. A 103 (1999) 8483.
[20] Scientific Computing & Modelling NV, Vrije Universiteit, Theoretical Chemistry, De Boelelaan 1083, 1081 HV, Amsterdam, The Netherlands.
[21] J. Baerends, A. Bérces, C. Bo, P.M. Boerrigter, L. Cavallo, L. Deng, R.M. Dickson, D.E. Ellis, L. Fan, T.H. Fischer, C. Fonseca Guerra, S.J.A. van Gisbergen, J.A. Groeneveld, O.V. Gritsenko, F.E. Harris, P. van den Hoek, H. Jacobsen, G. van Kessel, F. Kootstra, E. van Lenthe, V.P. Osinga, P.H.T. Philipsen, D. Post, C.C. Pye, W. Ravenek, P. Ros, P.R.T. Schipper, G. Schreckenbach, J.G. Snijders, M. Sola, D. Swerhone, G. te Velde, P. Vernooijs, L. Versluis, O. Visser, E. van Wezenbeek, G. Wiesenekker, S.K. Wolff, T.K. Woo, T. Ziegler, ADF 1999 program; E.J. Baerends, D.E. Ellis, P.

Ros, Chem. Phys. 2, 41 (1973); L. Versluis, T. Ziegler, J. Chem. Phys. 322, 88 (1988); G. te Velde, E.J. Baerends, J. Comput. Phys. 99 (1), 84 (1992); C. Fonseca Guerra, J.G. Snijders, G. te Velde, E.J. Baerends, Theor. Chem. Acc. 99, 391 (1998).
[22] Y. Wang, J.P. Perdew, Phys. Rev. B 43 (1991) 8911.
[23] L. Jeloaica, V. Sidis, Chem. Phys. Lett. 300 (1999) 157.
[24] I.F. Silvera, Rev. Modern Phys. 52 (1980) 393.
[25] W. Langel, D.L. Price, R.O. Simmons, P.E. Sokol, Phys. Rev. B. 38 (1988) 11275.
[26] A.D. Novaco, Phys. Rev. B: Condens. Matter 46 (1992) 8178.
[27] A.D. Novaco, Phys. Rev. Lett. 60 (1988) 2058.
[28] A.D. Novaco, J.P. Wroblewski, Phys. Rev. B: Condens. Matter 39 (1989) 11364.
[29] J.M. Nicol, J. Eckert, J. Howard, J. Phys. Chem. (1998).